

## NUMERICAL STUDY OF LAMINAR AND TURBULENT FLOW WITH RADIATIVELY PARTICIPATING MEDIA

by

**Roberto ALVARADO-JUAREZ<sup>a,b</sup>, Jesus XAMAN<sup>a</sup>,  
Irving HERNANDEZ-LOPEZ<sup>c</sup> and Gabriela ALVAREZ<sup>a</sup>**

<sup>a</sup>National Center for Research and Technology Development (CENIDET),  
Cuernavaca, Morelos, Mexico

<sup>b</sup>Technological University of the Center of Veracruz, Cuitlahuac, Veracruz, Mexico.

<sup>c</sup>Institute of Technology of Emiliano Zapata (ITZ), Zacatepec de Hidalgo, Morelos, Mexico

Original scientific paper  
<https://doi.org/10.2298/TSCI171010309A>

*The effect of radiation of a gray gas in a square cavity with double diffusive natural convection is presented. The regime flow studied range from a thermal Rayleigh number of  $10^4$  to  $10^{11}$  and buoyancy ratio from 0.5 to 2.0. The governing equations of fluid-flow, heat transfer and radiative transfer equation are solved by the finite volume method. The results show the effect of radiatively participating media plays an important role in the heat and mass transfer study doing oblique stratification. The velocity and turbulent viscosity increases about 80% and 22%, respectively, and decreases the convective Nusselt number 13%. The increase of buoyancy ratio increases the mass transfer until 26%. Finally, a practical correlation for computing the convective and radiative Nusselt numbers as well as the Sherwood number is proposed.*

Key words: radiative heat transfer, double diffusive convection, mass transfer, turbulent flow

### Introduction

Conjugate heat and mass transfer by natural convection is present in several engineering problems like nuclear reactors, combustion, drying process, solar still devices, electronics devices, thermal comfort, *etc* [1-4]. In the last 25 years, the study of conjugate heat transfer with participating media has increased due to the advances in computational technology, especially in those topics of natural convection and radiation [5-10] and natural heat and mass transfer convection [11-13].

Fusegi and Farouk [14] demonstrated the heat transfer increases due to the thermal radiation, and the gas radiation reduces the heat transfer to the walls. Mezrhab *et al.* [15] observed that radiation modifies the thermal field and the opacity of the fluid does not have an influence on the mass transfer. Meftah *et al.* [16, 17] concluded the gas radiation weakens the global heat transfer across the cavity and made inclined iso-values lines. Ibrahim and Lemonnier [18] concluded that gas radiation modifies the structure of the velocity and thermal fields. The results of Abidi *et al.* [19] revealed the for thermally dominated flow, the increasing of radiation results in a change from a multicellular inner core to a unicellular one, while for solutally dominated flow, an inverse transition from a unicellular one to a multi-cell pattern occurs. Lari and Gandjalikhan Nassab [20] concluded that when the radiation heat transfer becomes dominant disturbance is

<sup>\*</sup>Corresponding author, e-mail: ralvarado@uaem.mx, robertoalvaradoj@gmail.com

clearly seen in the heat flux contours. Moufekkir *et al.* [21, 22] observed that volumetric radiation accelerates the boundary-layer and that the isotherms and iso-concentrations are inclined in the cavity. The results of the study of Jena *et al.* [23] revealed the scattering albedo does not affect the energy transport of the system. Kolsi *et al.* [24] showed the flow structure is modified when the radiation-conduction varies. Ibrahim *et al.* [25] demonstrate that the combination of wall radiation and fluid radiation increases the level of turbulence accelerating the flow motion along the horizontal walls. Ansari and Gandjalikhan Nassab [26] concluded that the gas-flow must be considered as a radiating medium and must be taken into account in all the mechanism of heat transfer.

From this review, it is clear that there is a need to analyze the effect of heat and mass transfer in in turbulent regime flow, considering the working fluid radiatively participating media, due to the wide range of applications. Therefore, the goal of this research is to study numerically a square cavity with conjugate heat and mass transfer in laminar and turbulent regime flow, with radiatively participating media at low temperatures and a gray gas.

#### Physical model

The problem considered is the study of the conjugate heat and mass transfer in a square cavity heated differentially as shown in fig. 1. The cavity contains a perfect mixture of air and water vapor assumed as a gray gas, absorbing-emitting and non-scattering fluid. The left and right walls are maintained isothermal at high,  $T_h$ , and low,  $T_c$ , temperature, respectively. These walls are also considered with two constant concentration at each wall,  $C_h > C_c$ . The top and bottom walls are adiabatic and impermeable. All the thermophysical properties are evaluated at the average temperature  $T_0 = (T_h + T_c) / 2$  with the correlation reported in [27, 28]. The inner surfaces of the cavity are assumed gray, diffuse and opaque.

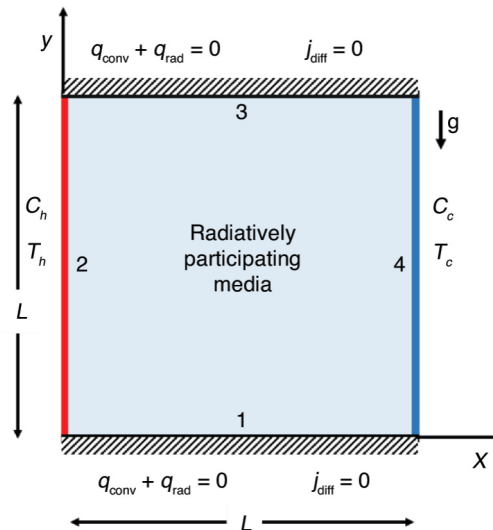


Figure 1. Physical model of the square cavity with double-diffusive convection

#### Governing equations and boundary conditions for the fluid-flow

The steady-state governing equations inside the cavity (fig. 1) are the mass, momentum, energy and concentration of water vapor equations for natural convection:

$$\frac{\partial}{\partial x_i}(\rho u_i) = 0 \quad (1)$$

$$\frac{\partial(\rho u_i u_i)}{\partial x_i} = -\frac{\partial P}{\partial x_i} + \frac{\partial}{\partial x_j} \left[ \mu \left( \frac{\partial u_i}{\partial x_j} + \frac{\partial u_j}{\partial x_i} \right) - \rho \overline{u_i u_j} \right] - \rho [\beta_T (T - T_0) + \beta_C C - C_0] g, \quad (2)$$

$$\frac{\partial(\rho u_i T)}{\partial x_i} = -\frac{1}{C_p} + \frac{\partial}{\partial x_i} \left[ \lambda \frac{\partial T}{\partial x_i} - C_p \rho \overline{u_i T} \right] - \frac{1}{C_p} \frac{\partial q_{rad,i}}{\partial x_i} \quad (3)$$

$$\frac{\partial(\rho u_j C)}{\partial x_j} = \frac{\partial}{\partial x_j} \left[ \rho D_{w,a} \frac{\partial C}{\partial x_j} - \rho u_j C \right] \quad (2)$$

For the turbulence model  $k-\omega$ , the turbulent kinetic energy and the specific dissipation of the turbulent model PDH+D were defined by Peng *et al.* [29, 30]:

$$\frac{\partial(\rho u_i k)}{\partial x_i} = \frac{\partial}{\partial x_i} \left[ \left( \mu + \frac{\mu_t}{\sigma_k} \right) \frac{\partial k}{\partial x_i} \right] + P_k + f_g G_k - c_k f_k \rho k \omega \quad (5)$$

$$\frac{\partial(\rho u_i \omega)}{\partial x_i} = \frac{\partial}{\partial x_i} \left[ \left( \mu + \frac{\mu_t}{\sigma_\omega} \right) \frac{\partial \omega}{\partial x_i} \right] + c_{\omega 1} f_1 P_k \left( \frac{\omega}{k} \right) + c_{\omega 3} G_k \left( \frac{\omega}{k} \right) - c_{\omega 2} f_2 \rho \omega^2 + D \quad (6)$$

The non-slip condition is applied for the hydrodynamic boundary conditions at the solid walls ( $u = v = 0$ ). The top and bottom walls are adiabatic ( $-\lambda \partial T / \partial y + q_{rad} = 0$ ) and impermeable ( $\partial C / \partial y = 0$ ). While the other two have constant temperature and concentration ( $T = T_h$  and  $C = C_h$  at  $x = 0$  and  $T = T_c$  and  $C = C_c$  at  $x = L$ , with  $T_c < T_h$  and  $C_c < C_h$ ). The turbulent kinetic energy on the wall is zero ( $k = 0$ ). The specific dissipation on the wall is  $\omega = 6\mu / (C_2 \rho x_{wall}^2)$  at  $x = 0$  and  $x = L$  and  $\omega = 6\mu / (C_2 \rho y_{wall}^2)$  at  $y = 0$  and  $y = L$ . Results presented for fluid flow are in stream function defined as  $\partial \Psi / \partial x = -v$  and  $\partial \Psi / \partial y = u$

#### Radiative transfer equation and boundary conditions

The radiative source term  $\partial q_{rad,i} / \partial x_i$  in the energy eq. (3) is related to the local radiative intensity and the intensity of radiation by [31]:

$$\frac{\partial q_{rad,i}}{\partial x_i} = \kappa \left( 4\pi I_b(\vec{r}) - \int_{4\pi} I(\vec{r}, \hat{s}) d\Omega \right) \quad (7)$$

$$\frac{dI(\vec{r}, \hat{s})}{ds} = \kappa [I_b(\vec{r}) - I(\vec{r}, \hat{s})] \quad (8)$$

The radiative boundary condition for diffuse reflecting and emitting surfaces is:

$$I(\vec{r}, \hat{s}) = \varepsilon^*(\vec{r}) I_b(\vec{r}) + \frac{\rho^*(\vec{r})}{\pi} \int_{\hat{s} \cdot \hat{n} < 0} I(\vec{r}, \hat{s}') |\hat{n} \cdot \hat{s}'| d\Omega' \quad (9)$$

#### Heat and mass transfer

The total heat transfer, at the vertical walls, is given by the Nusselt number; this involves the contribution of the convective and radiative Nusselt numbers, meanwhile the total mass transfer, across the active walls, is given by the Sherwood number as and can be expressed:

$$Nu_{conv} = \frac{-\lambda}{q_{cond} L} \int_0^L \frac{\partial T}{\partial x} dy \quad (10)$$

$$Nu_{rad} = \frac{1}{q_{cond} L} \int_0^L q_{rad} dy \quad (11)$$

$$Nu_{total} = Nu_{conv} + Nu_{rad} \quad (12)$$

$$q_{cond} = \frac{\lambda(T_h - T_c)}{L} \quad (13)$$

$$Sh = \frac{\rho D_{w,a}}{j_{diff} L} \int_0^L \frac{\partial C}{\partial x} dy \quad (14)$$

$$j_{\text{diff}} = \frac{\rho D_{\text{wa}}(C_h - C_c)}{L} \quad (15)$$

### Numerical method

The 2-D governing eqs. (1)-(6) were solved numerically using the finite-volume method [32] and the coupling of the continuity and momentum equations were done with the SIMPLEC algorithm [33]. The convective terms were approximated by the SMART scheme [34-36] and the diffusive terms were approximated by the central differential scheme. The system of algebraic equations was solved with the MSIP method [37]. A non-uniform staggered grid was used. The RTE equation (8) was solved using the finite-volume method [38, 39] and the STEP scheme was used in the algebraic equations obtained from eq. (8). The coupling between natural convection and radiation of the participating media in the cavity were solved using an iterative approach. The coupling of the effect of RTE on the turbulent heat fluxes and the mass fluxes was done through the local temperature that has the effects of participating media after solving the RTE.

For ensuring the accuracy of the numerical results, several grids were tested to show the effect of the spatial grid on the average Nusselt number (convective and radiative), average Sherwood number, and the maximum turbulent viscosity. The grids tested varied from  $71 \times 71$  nodes to  $141 \times 141$  nodes in  $x$ - and  $y$ - direction, respectively. The parameters used for the test were  $Ra = 10^{11}$ ,  $T_h = 313.15$  K,  $T_c = 293.15$  K,  $RH = 50\%$ , and  $N = 2$  with radiatively participating media. From the test, it was observed that for grids higher than  $121 \times 121$  nodes, the difference is less than 1% for all variables. For the dependence directional, the angular grid varied from  $6 \times 6$  to  $34 \times 34$  nodes in  $\theta$  and  $\phi$  directions. The results showed that for grids higher than  $14 \times 14$  the difference in the radiative source term is less than 1%. From the numerical test, it was confirmed that the numerical grid of  $131 \times 131$  ( $x, y$  position) and  $18 \times 18$  ( $\theta, \phi$  direction) ensures a grid independent solution (fig. 2). The convergence criterion was set at  $10^{-10}$ .

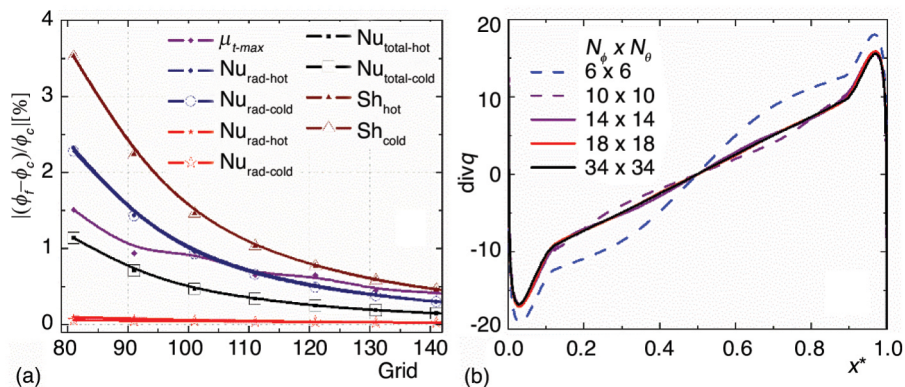


Figure 2. (a) Spatial grid independence, (b) directional grid independence (for colour image see journal website)

### Verification and validation of the numerical code

In order to verify and validate the numerical code developed, the general problem is reduced to three cases reported in the literature. The first case is the verification of the coupling of heat and mass transfer in a square cavity reported by Xaman *et al.* [40]. The comparison was done for the  $Nu$  and  $Sh$  reported in the tab. 1 in [40] with a maximum error of 1.8% for  $N = -0.9$ . The second case is the validation of heat transfer with turbulent flow in a square cavity reported by

Ampofo and Karayiannis [41]. The results compared were the dimensionless value of  $T^*$ ,  $v^*$ ,  $k^*$  and Nu for  $Ra_T = 1.58 \times 10^9$  and a good agreement was obtained. Finally, the third case is the verification of the coupling of natural convection with radiatively participating media (RH = 50%) in a square cavity with turbulent flow reported by Ibrahim *et al.* [25]. The comparison was with the results of tab. 3 reported in [25] obtaining a maximum difference percentage of 4.6% for the case of radiative Nusselt number in the hot wall, and the average difference percentage was 2.3%.

### Results and discussion

To analyze the characteristics of the flow, temperature and concentration fields, the steady-state solution are presented for the range of  $10^4 \leq Ra_T \leq 10^{11}$ . The hot and cold wall are maintained at a constant value of  $T_h = 313.15$  K and  $T_c = 293.15$  K, and the buoyancy ratio is considered for the values of  $N = 0.5, 1$ , and 2. The thermophysical properties are computed at the pressure, average temperature and RH of 50% ( $\rho = 1.148$  kg/m<sup>3</sup>,  $\mu = 1.824 \cdot 10^{-5}$  kg/ms,  $\lambda = 2.615 \cdot 10^{-2}$  W/mK,  $C_p = 1029.75$  J/kgK,  $D_{w,a} = 2.593 \cdot 10^{-5}$  m<sup>2</sup>/s) with this value the concentration of  $C_h$  and  $C_c$  was computed with the average absorption coefficient of 0.1 [25]. As the effect of oppo-

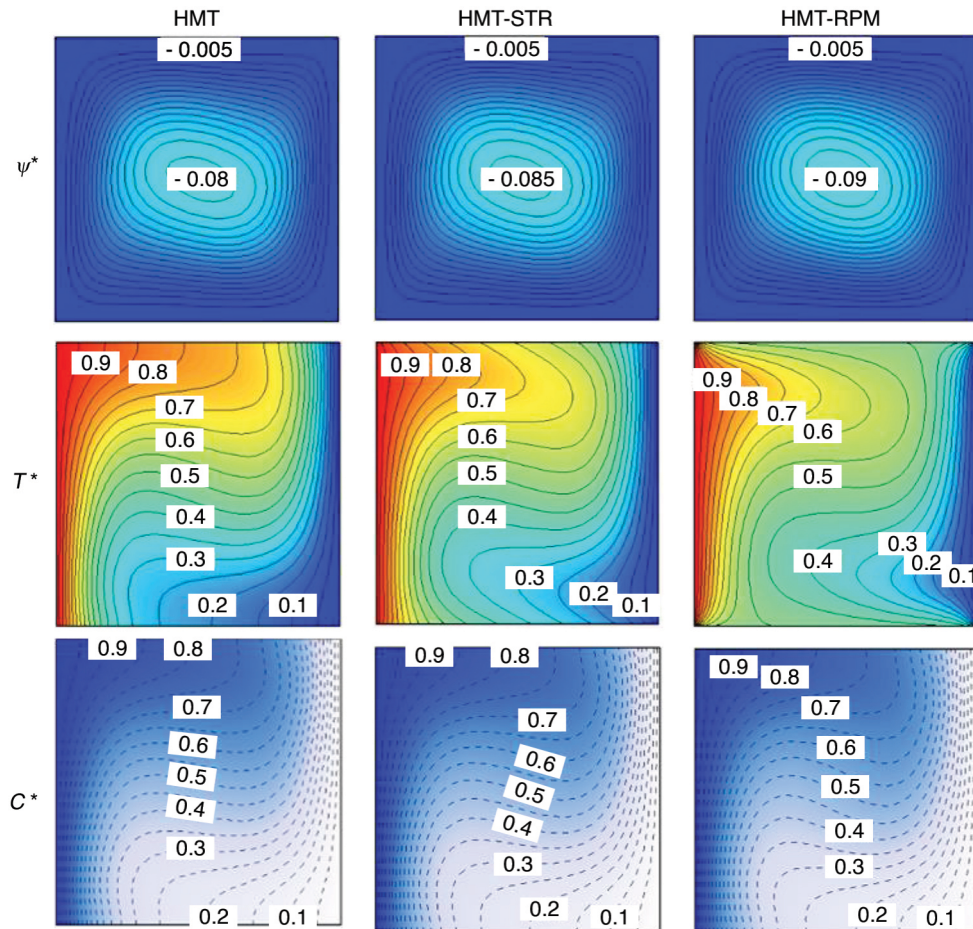


Figure 3. Comparison of  $\psi^*$ ,  $T^*$ , and  $C^*$ , for  $Ra_T = 10^4$  and  $N = 1$

site flow with different values of concentration and buoyancy ratio was analyzed in laminar regime flow by others researches, just the results of assisted flow is analyzed for laminar and turbulent flow of heat and mass transfer for the cases: Case 1 only considers the heat and mass transfer (HMT) of the gray gas, Case 2 considers the HMT with surface thermal radiation (HMT-STR); and Case 3 considers the HMT with radiatively participating media (HMT-RPM).

Figure 3 shows the comparison of the contour of streamlines, isotherms and iso-concentration of water vapor for  $Ra_r = 10^4$  and  $N = 1$  for the cases considered. Streamlines show that a clockwise movement is present; when the radiation is present the streamlines increase in the core of the cavity 6.25% for STR and 12.5% for RPM. Isotherms show that the highest gradi-

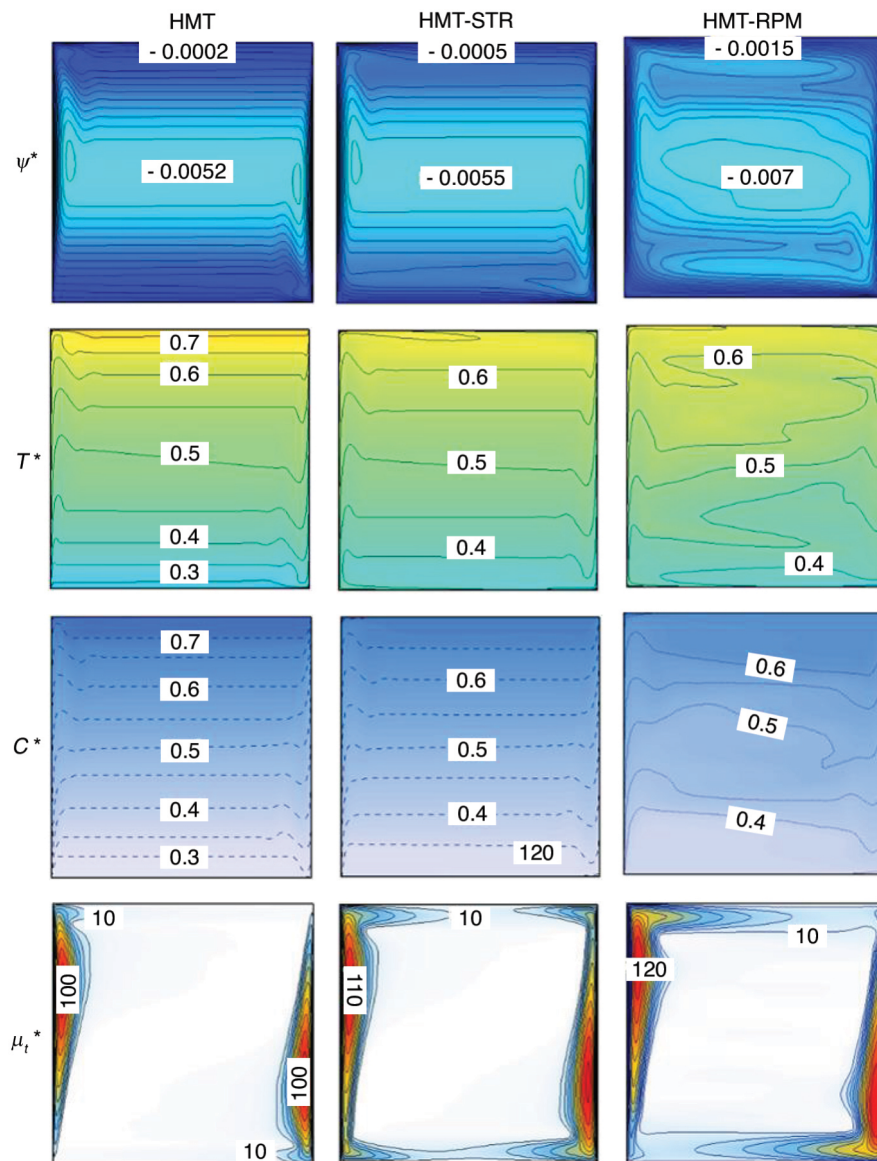


Figure 4. Comparison of  $\psi^*$ ,  $T^*$ ,  $C^*$  and  $\mu_t^*$ , for  $Ra_r = 10^{11}$  and  $N = 1$

ents are near the vertical walls; for the case of HMT the isotherms are normal to the adiabatic wall. The STR produces inclined and distributed isotherms along the adiabatic walls, meanwhile for the case RPM the inclined isotherms are concentrated near the corners, the higher gradients of temperature are present in this case. The iso-concentration of water vapor shows that there is not significant changes in the patterns for the laminar flow due to, as it is observed in eq. (4), there is not a direct effect of the radiative source term in the equation of concentration of water vapor. It is observed that the symmetry in the flow pattern is present.

Figure 4 shows the comparison of the streamlines, isotherms, iso-concentration and turbulent viscosity for  $Ra_r = 10^{11}$  and  $N = 1$ . The streamlines show that a symmetric clockwise movement is present; the presence of STR increases the velocity of the fluid and the gradients near the horizontal walls about 10% with respect the case HMT, two cells in the same sense of the main vortex are near the active walls. The presence of RPM increases even more the velocity of the fluid until a 48% with respect the case of HMT and two cells moving in the same sense of the main vortex are near the top and bottom walls. For both case STR as for case RPM, the radiation breaks the symmetry of the problem.

The isotherms for HMT show thermal stratification with almost uniform gradients along the vertical centerline, in the middle of the cavity there is an inclined isotherm. When the STR is considered, the temperature gradients are increased in the boundary-layer and in the rest of the cavity thermal occur stratification. Moreover, the RPM disappears the thermal stratification and increases the temperature gradients in the boundary-layer. The iso-concentration of water vapor presents a similar behavior as the isotherms. The turbulent viscosity shows a typical behavior for the case of HMT in the vertical walls. The presence of STR increases the turbulent viscosity approximately 10%, this is present in the isothermal, bottom and 2/3 parts of the top walls. The RPM increases the turbulent viscosity approximately 20% and it is present in all the walls of the cavity. It is observed that for the case of STR, the increases of the turbulent viscosity and velocity is due to the fluid increases the temperature. When the RPM is considered, the fluid increases the turbulent viscosity even more because the fluid gains energy not only in the boundary, but also within itself due to the capability to absorb energy.

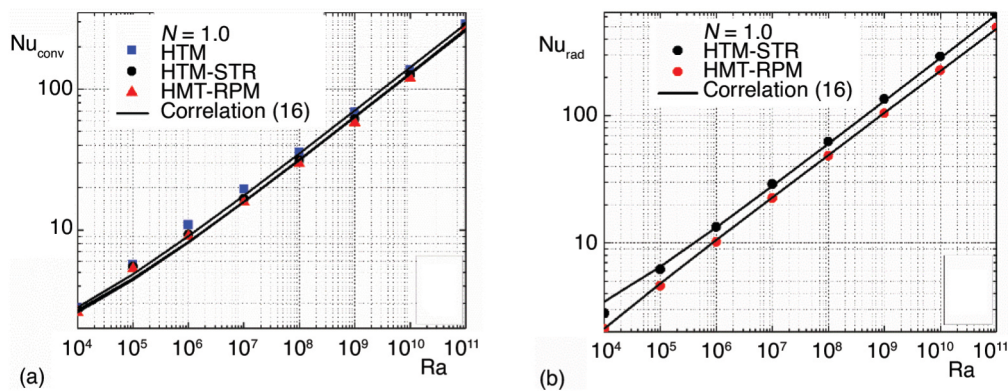


Figure 5. Comparison of (a)  $Nu_{conv}$  and (b)  $Nu_{rad}$  for  $N = 1$

Figure 5 shows the comparison of the mean convective and radiative Nusselt numbers in the hot wall for  $N=1.0$ , the range of  $10^4 \leq Ra_r \leq 10^{11}$  and the cases of HMT, HMT-STR and HMT-RPM. Figure 5(a) shows that as the  $Ra$  increases the  $Nu_{conv}$  increases significantly. It is clear that the radiative heat exchange decreases the heat transfer by convection because the  $Nu_{conv}$  for the case HMT is higher than the cases HMT-STR and HMT-RPM. For the case of HMT-STR this

reduction is about 9%, for the case of HMT-RPM the convective heat transfer decreases about 13%, the higher decreases is due to the fluid increases the temperature due to the absorption of thermal energy. Figure 5(b) shows the comparison of the  $Nu_{rad}$  for the cases HMT-STR and HMT-RPM, it is clear that the presence of RPM decreases the radiative heat transfer about 23%, due to the gray gas absorb part of the energy transferred from the hot wall to the cold wall.

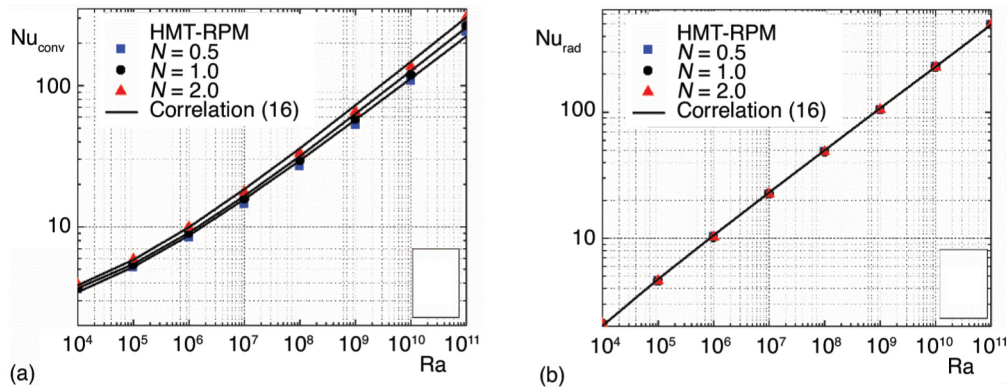


Figure 6. Comparison of (a)  $Nu_{conv}$  and (b)  $Nu_{rad}$  for the case of HMT-RPM

Figure 6 shows the comparison of the mean convective and radiative Nusselt number in the hot wall for the case of HMT-RPM, the range of  $10^4 \leq Ra_r \leq 10^{11}$  and the cases  $N = 0.5, 1.0$  and  $2.0$ . Figure 6(a) shows that as the  $Ra$  increases the  $Nu_{conv}$  increases too. The increase of  $N$  increases the convective heat transfer, this increases is about 7% and 19% for  $N = 1.0$  and  $N = 2.0$ , respectively compared to the case of  $N = 0.5$ . In fig. 6(b) it is observed that the increases of  $N$  do not have effect in the radiative heat transfer due to in the equation of concentrations it is not considered the gradients of temperature.

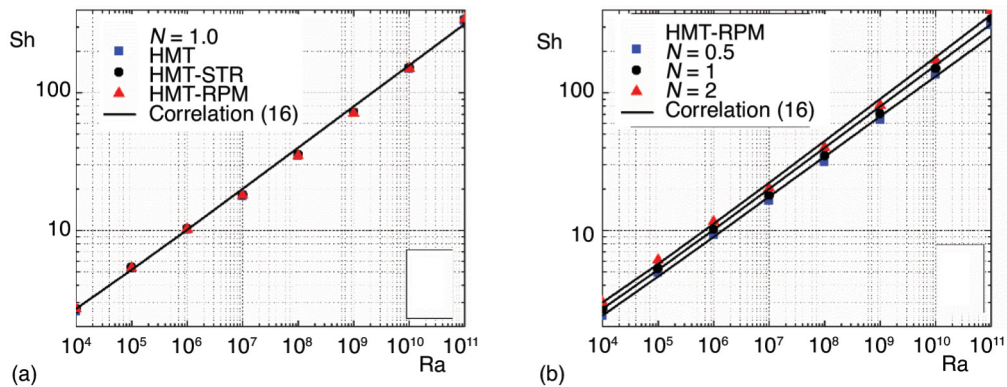


Figure 7. Comparison of the  $Sh$  for the case of (a) with and without radiation and (b) for different values of  $N$

Figure 7 shows the comparison of the Sherwood number for cases of HMT, HMT-STR and HMT-RPM and for different values of  $N$ . In fig. 7(a) it is observed that there is not difference in the Sherwood number for the cases mentioned, this is due to in this case the Soret and Dufour effects are not considered, these effects are considered in a future publication. The radiative exchange process does not have effect on the mass transfer for the cases presented in the manuscript. Figure 7(b) presents the effect of the Sherwood number with the variation of  $N$ , as  $N$

increases the Sherwood number increases about 10 and 26% for  $N=1$  and  $N=2$ , respectively, compared to  $N=0.5$ .

From figs. 5-7, a practical correlation to compute for the convective and radiative and Nusselt number as well as the Sherwood number is proposed. The correlation proposed, using least square regression, is (16) and the corresponding coefficients a, b and c are showed in tab. 1.

$$f(Ra) = a + bRa_c \quad (16)$$

**Conclusions**

The numerical study of the double-diffusive natural convection in a square cavity was presented. The working fluid was humid air considered as a gray gas that was radiatively participating. The parameters considered were  $T_h = 313.15$  K,  $T_c = 293.15$  K, HR = 50 %,  $0.5 \leq N \leq 2.0$ , and  $10^4 \leq Ra_r \leq 10^{11}$ . The results obtained were presented in condition of low gradient of temperature and low concentration of humidity. For modelling the turbulence, the PDH + D  $k-\omega$  model was used and for solving the RTE the finite volume method was used. Based on the results, the following conclusions were obtained:

- Non-symmetry was presented in the isotherms both laminar and turbulent flow. Although the iso-concentrations were not affected in laminar flow, in turbulent flow the iso-concentrations showed a tendency not to be stagnant in the center of the cavity.
- The radiatively participating media increased the velocity of the fluid and the turbulent viscosity until 48% and 20%, respectively.
- The increase of buoyancy ratio increased the velocity and the turbulent viscosity until 80% and 22%, respectively.
- The radiatively participating media decreased the  $Nu_{conv}$  about 13% with respect to the case without radiation due to the participating media increases the temperature of the fluid.
- The increase of buoyancy ratio increased the mass transfer until 26%.
- Finally, a practical correlation for computing the convective, radiative and the Sherwood number was proposed with an average percentage absolute difference of 3.2%.

**Acknowledgment**

R. Alvarado-Juarez thanks to CONACYT, whose financial support made this work possible.

**Nomenclature**

$C$	– concentration of species, [kgkg <sup>-1</sup> ]	$L$	– length of the cavity, [m]
$C_p$	– specific heat, [Jkg <sup>-1</sup> K <sup>-1</sup> ]	$j$	– mas flux [kgm <sup>-2</sup> s <sup>-1</sup> ]
$D_{w,a}$	– mass diffusivity, [m <sup>2</sup> s <sup>-1</sup> ]	$N$	– buoyancy ratio [ = $\beta_c C / (\beta_r T)$ ], [-]
$g$	– gravity, [9.81 ms <sup>-2</sup> ]	$Nu$	– nusselt number ( = $q/q_{cond}$ ), [-]
$I$	– radiation intensive, [Wm <sup>2</sup> sr <sup>-1</sup> ]	$P$	– pressure, [Pa]
$k$	– turbulent kinetic energy, [m <sup>2</sup> s <sup>-2</sup> ]	$q$	– heat flux, [Wm <sup>-2</sup> ]

**Table 1. Coefficients of the correlation (16)**

$f(Ra)$	Case	a	b	c
Figure 5				
$Nu_{conv}$	HMT	0.8600	0.1129	0.3100
	HTM-STR	1.0000	0.0960	0.3130
	HMT-RPM	0.8500	0.1010	0.3100
$Nu_{rad}$	HMT-STR	0.8600	0.1129	0.3400
	HMT-RPM	-0.2400	0.1129	0.3300
Figure 6				
	$N = 0.5$	1.7000	0.1110	0.3000
	$N = 1.0$	2.0000	0.0950	0.3120
	$N = 2.0$	2.0000	0.1010	0.3160
	$N = 0.5$	-0.3500	0.1130	0.3310
	$N = 1.0$	-0.3500	0.1130	0.3310
	$N = 2.0$	-0.3500	0.1130	0.3310
Figure 7				
Sh	HMT	0.2200	0.1550	0.3010
	HTM-STR	0.2200	0.1550	0.3010
	HMT-RPM	0.2200	0.1550	0.3010
Sh	$N = 0.5$	0.1000	0.1550	0.2930
	$N = 1.0$	0.2200	0.1550	0.3010
	$N = 2.0$	0.3800	0.1550	0.3070

Ra <sub>t</sub>	– thermal Rayleigh number [= $g\beta_T(T_i - T_b)L^3/(\alpha)$ ], [–]	$\beta_c$	– concentration expansion coefficient (= $1/C_0$ ), [ $\text{kg}^{-1}\text{m}^3$ ]
Ra <sub>m</sub>	– mass Rayleigh number [= $g\beta_M(C_i - C_b)L^3/(D_{wa})$ ], [–]	$\varepsilon^*$	– emittance, [–]
Sh	– Sherwood number (= $CL/D_{wa}$ ), [–]	$\kappa$	– absorption coefficient, [ $\text{m}^{-1}$ ]
T	– temperature, [K]	$\lambda$	– thermal conductivity, [ $\text{Wm}^{-1}\text{K}^{-1}$ ]
u, v	– velocities, [ $\text{ms}^{-1}$ ]	$\mu$	– dynamic viscosity, [ $\text{kgm}^{-1}\text{s}^{-1}$ ]
$x, y$	– dimensional co-ordinates, [m]	$\mu_t$	– turbulent viscosity, [ $\text{kgm}^{-1}\text{s}^{-1}$ ]
$x^*, y^*$	– dimensionless co-ordinates, [–]	$\rho$	– density, [ $\text{kgm}^{-3}$ ]
<i>Greek symbols</i>		$\rho^*$	– reflectance, [–]
$\alpha$	– thermal diffusivity (= $\lambda/\rho C_p$ ), [ $\text{m}^2\text{s}^{-1}$ ]	$\nu$	– kinematic viscosity, [ $\text{m}^2\text{s}^{-1}$ ]
$\beta_T$	– thermal expansion coefficient (= $1/T_0$ ), [ $\text{K}^{-1}$ ]	$\omega$	– turbulence frequency, [ $\text{s}^{-1}$ ]
		$\Psi$	– stream Function, [–]

## References

- [1] Goldstein, R. J., et al., Heat Transfer a Review of 2003 Literature, *Int. J. Heat Mass Transfer*, 49 (2006), 3-4, pp. 451-534
- [2] Goldstein, R. J., et al., Heat Transfer a Review of 2004 Literature, *Int. J. Heat Mass Transfer*, 53 (2010), 21, 22, pp. 4343-4396
- [3] Risberg, D., et al., Computational Fluid Dynamics Simulation of Indoor Climate in Low Energy Buildings, Computational Set Up, *Thermal Science*, 21 (2017), 5, pp. 1985-1998
- [4] Dawood, H. K., et al., Forced, Natural and Mixed-Convection Heat Transfer and Fluid Flow in Annulus: a Review, *Int. Comm. Heat Mass Transfer*, 62 (2015), Mar., pp. 45-57
- [5] Yucel, A., et al., Natural Convection and Radiation in a Square Enclosure, *Numer. Heat Transfer, Part A: Applications*, 15 (1989), 2, pp. 261-278
- [6] Fusegi, T., et al., 3-D Natural Convection-Radiation Interaction in a Cube Filled with Gas-Soot Mixtures, *Proceedings, 3<sup>rd</sup> Int. Symp. Fire Safety Sci.*, Edinburgh, Scotland, 1991, pp. 365-374
- [7] Yucel, A., et al., Natural Convection of Radiating Fluid in a Square Enclosure with Perfectly Conducting Walls, *Sadhana*, 19 (1994), Oct., pp. 751-764
- [8] Draoui, A., et al., Numerical Analysis of Heat Transfer by Natural Convection and Radiation in Participating Fluids Enclosed in Square Cavities, *Numer. Heat Transfer, Part A: Applications*, 20 (1991), 2, pp. 253-261
- [9] Colomer, G., et al., Three-Dimensional Numerical Simulation of Convection and Radiation in a Differentially Heated Cavity Using the Discrete Ordinates Method, *Int. J. Heat and Mass Transfer* 47 (2004), 2, pp. 257-269
- [10] Lv, Y.-C., et al., Analytical Solution for the 1-D Heat Transfer Equations with Radiative Loss, *Thermal Science*, 21 (2017), S1, pp. s47-s53
- [11] Beghein, C., et al., Numerical Study of Double-Diffusive Natural Convection in a Square Cavity, *Int. J. Heat Mass Transfer*, 35 (1992), 4, pp. 833-846
- [12] Kadem, S., et al., Computational Analysis of Heat and Mass Transfer During Microwave Drying of Timber, *Thermal Science*, 20 (2016), 5, pp. 1447-1455
- [13] Abidi, A., et al., Effect of Heat and Mass Transfer through Diffusive Walls on Three-Dimensional Double Diffusive Natural Convection, *Numer. Heat Transfer, Part A: Applications*, 53 (2008) 12, pp. 1357-1376
- [14] Fusegi, T., Farouk, B., Laminar and Turbulent Natural Convection-Radiation Interactions in a Square Enclosure Filled with a Nongray Gas, *Numer. Heat Transfer, Part A: Applications*, 15 (1989), 3, pp. 303-322
- [15] Mezrhab, A., et al., Numerical Study of Double-Diffusion Convection Coupled to Radiation in a Square Cavity Filled with a Participating Gray Gas, *J. Phys. D.: Appl. Phys.*, 41 (2008), 9, 195501
- [16] Meftah, S., et al., Coupled Radiation and Double Diffusive Convection in Nongray Air-CO<sub>2</sub> and Air-H<sub>2</sub>O Mixtures in Cooperating Situations, *Numer. Heat Transfer, Part A: Applications*, 56 (2009), 1, pp. 1-19
- [17] Meftah, S., et al., Comparative Study of Radiative Effects on Double Diffusive Convection in Nongray Air-CO<sub>2</sub> Mixtures in Cooperating and Opposing Flow, *Math. Probl. Eng.*, 2015 (2015), ID 586913
- [18] Ibrahim, A., Lemonnier, D., Numerical Study of Coupled Double-Diffusive Natural Convection and Radiation in a Square Cavity Filled with a N<sub>2</sub>-CO<sub>2</sub> Mixture, *Int. Comm. Heat Mass Transfer*, 36 (2009), 3, pp. 197-202
- [19] Abidi, A., et al., Effect of Radiative Heat Transfer on Three-Dimensional Double Diffusive Natural Convection, *Numer. Heat Transfer, Part A: Applications*, 60 (2011), 9, pp. 785-809
- [20] Lari, K., Gandjalikhan Nassab, S.A., Modeling of the Conjugate Radiation and Conduction Problem in 3-D Complex Multi-Burner Furnace, *Thermal Science*, 16 (2012), 4, pp. 1187-1200

- [21] Moufekkik, F., et al., Combined Double-Diffusive Convection and Radiation in a Square Enclosure Filled with Semitransparent Fluid, *Comp. Fluids*, 36 (2012), Oct., pp. 172-178
- [22] Moufekkik, F., et al., Study of Double-Diffusive Natural Convection and Radiation in an Inclined Cavity using Lattice Boltzmann Method, *Int. J. Therm. Sci.*, 63 (2013), Jan, pp. 65-86
- [23] Jena, S. K., et al., Interaction of Participating Medium Radiation with Thermosolutal Convection A critical Appraisal, *Heat Transfer Asian Research*, 44 (2015), 1, pp. 39-65
- [24] Kolsi, L., et al., Combined Radiation-Natural Convection in Three-Dimensional Vertical Cavities, *Thermal Science*, 15 (2011), 2, pp. 327-S339
- [25] Ibrahim, A., et al., Coupling Natural Convection with Radiation in an Air-Filled Differentially Cavity at  $Ra = 1.5 \times 10^9$ , *Comp. Fluids*, 88 (2013), 12, pp. 115-125
- [26] Ansari, A. B., Gandjalikhhan Nassab, S. A., Forced Convection of Radiating Gas Over an Inclined Backward Facing Step using the Blocked-Off Method, *Thermal Science*, 17 (2013), 3, pp. 773-786
- [27] Alvarado-Juarez, R., et al., Numerical Study of Conjugate Heat and Mass Transfer in a Solar Still Device, *Desalination*, 325 (2013), Sept., pp. 84-94
- [28] Alvarado-Juarez, R., Study of the Heat and Mass Transfer in a Room with a Radiatively Participating Media, Ph. D. Thesis, CENIDET, Morelos, Mexico, 2016
- [29] Peng, S., et al., Performance of Two-equation Models for Numerical Simulation of Ventilation Flows, *Proceedings*, 5<sup>th</sup> Int. Conf. on Air Distributions in Rooms, Yokohama, Japan, 1996, Vol. 2, pp. 153-160
- [30] Peng, S., et al., A Modified Low-Reynolds-Number  $\omega$ - $k$  Model for Recirculating Flows, *J. Fluid Eng.*, 119 (1997), 4, pp. 867-875
- [31] Modest, M. F., *Radiative Heat Transfer*, Academic Press, New York, USA, 2003
- [32] Patankar, S. V., *Numerical Heat Transfer and Fluid Flow*, Taylor and Francis, London, 1980
- [33] Van Doormal, J. P., Raithby, G. D., Enhancement of the SIMPLE Method for Predicting Incompressible Fluid Flows, *Numer. Heat Transfer, Part A: Applications*, 7 (1984), 2, pp. 147-163
- [34] Gaskell, P. H., Lau, A. K. C., Curvature-Compensated Convective Transport: SMART, a New Boundedness-Preserving Transport Algorithm, *Int. J. Numer. Meth. Fluids*, 8 (1988), 6, pp. 617-641
- [35] Darwish, M. S., Moukalled, F., Normalized Variable and Space Formulation Methodology for High-Resolution Schemes, *Numer. Heat Transfer, Part B: Fundamentals*, 26 (1994), 1, pp. 79-96
- [36] Darwish, M. S., Moukalled, F., The Normalized Weighting Factor Method: a Novel Technique for Accelerating the Convergence of High-Resolution Convective Schemes, *Numer. Heat Transfer, Part B: Fundamentals*, 30 (1996), 2, pp. 217-237
- [37] Schneider, G. E., Zedan, M., A Modified Strongly Implicit Procedure for the Numerical Solution of Field Problems, *Numer. Heat Transfer*, 4 (1981), 1, pp. 1-19
- [38] Chui, E. H., Modeling of Radiative Heat Transfer in Participating Media by the Finite Volume Method, Ph. D. Thesis, University of Waterloo, Waterloo, Ont., Canada, 1990
- [39] Chai, J. C., A Finite-Volume Method for Radiation Heat Transfer, Ph. D. Thesis, University of Minnesota, Minneapolis, Minn., USA, 1994
- [40] Xaman, J., et al., Effect of a Contaminant Source ( $CO_2$ ) on the Air Quality in a Ventilated Room, *Energy*, 36 (2011), 5, pp. 3302-3318
- [41] Ampofo, F., Karayiannis, T. G., Experimental Benchmark Data for Turbulent Natural Convection in an Air Filled Square Cavity, *Int. J. Heat Mass Transfer*, 46 (2003), 19, pp. 3551-3572